Analysis, auralization and reduction of electromagnetic excited audible noise for electrical vehicles

Analyse, Auralisierung und Reduktion elektromagnetisch erregter Geräusche bei elektrisch angetriebenen Fahrzeugen

David Franck[1], M. van der Giet, [1] Pascal Dietrich[2], Kay Hameyer[1], Michael Vorländer[2]

[1] *Institute of Electrical Drives, RWTH Aachen, Germany, Email: df@iem.rwth-aachen.de*

[2] *Institute of Technical Acoustics, RWTH Aachen, Germany, Email: pdi@akustik.rwth-aachen.de*

Abstract

Electric vehicles are probably going to take an important role in individual transportation within the next years. Although they are known for their lower noise emission compared to automobiles driven by a combustion engine, significant acoustic problems are reported recently. This can be explained by looking at their sound spectra. Opposed to the acoustic noise from a combustion engine, the electric motor itself radiates sound with disturbing single tones stemming from the temporal and spatial periodic electromagnetic forces in the airgap. In the case of full electric vehicle no masking of those single tones by broadband noise sources as in the case of combustion engines can be expected. Therefore, it is essential to develop a fast simulation and measurement based methodology, by which the designer is able to analyze, assess, and optimize electrical drive trains in variable operation conditions. This involves the physical domains: electromagnetics, structural dynamics and acoustic radiation of air-borne sound. The developed methodology is novel in the sense that it uses a persistent decomposition into Fourier basis functions in the spatial domain of the forces acting at the airgap of the stator bore. In addition, fast analytical models are used whenever suitable. This is especially the case for the efficient calculation of the airgap field by a new numerical interpretation of the conformal mapping approach and a radiation model based on cylindrical harmonics. Thereby, not only a fast computer simulation is achieved but also a seamless coupling with measurement based determination of transfer functions, such as the modified operational TPA, relating the measured sound to the simulated magnetic forces becomes possible. Thus, the engineer is able to auralize the drive train of an electric vehicle in variable operating conditions. This is necessary, if e.g. a comparison with respect to the psychoacoutic performance of a complete standardized driving cycle is performed. Due to the fast computation, the optimization potential regarding the acoustic behavior can be exploited efficiently. Regarding the magnetic excitations, the electrical machine's noise can either be approached from the design or from the control. It is shown how the proposed methodology is used to achieve a significant lower noise level by slightly changing the magnet shapes. Controlling the machine current, active noise cancelation by injecting additional current harmonics can be implemented.

Introduction

Electric vehicles are required to have low levels of acoustic noise emission. Except some inconspicuous dynamic acoustic feedback of the current load conditions, there shall be no NVH (Noise, Vibration, Harshness) phenomena of the drive train perceivable inside of the vehicle interior. Although electrical drives are typically quieter than the combustion counter part, the characteristic is much different. Where the combustion engine has a broadband noise spectrum, the electrical machine causes single tones in the audible spectrum, due to the periodicity of the fields and forces typically generate single tones, which unfortunately often lie within a frequency band, in which the human ear is most sensitive [1].

Therefore, electric vehicles may be sensed more unpleasant compared to conventional vehicles driven by a combustion engine, despite their lower overall noise levels. From test drives, e.g. of the *Tesla Roadster* or the *smart fortwo electric drive*, a high frequency dominant acoustic noise

stemming from the electrical motor is reported [2][3]. Compared to electric railways this sound characteristics are not acceptable for automotive applications [4][5].

Permanent-magnet excited synchronous machines (PMSM) are employed in electric vehicles for their high torque density and efficiency. The increase of torque density typically goes together with an increase of air-gap flux-density level, leading to higher electromagnetic force excitation and ultimately to higher audible noise radiated by the machine.

For the reduction of audible noise of the electric vehicle, it is essential to pre-determine the acoustic behavior including the electromagnetic force excitation, structural dynamic behavior and sound transmission and radiation. Therefore, this paper describes a modular concept of transfer functions that allows a consistent description of acoustic phenomena inside the electric vehicle in terms of Fourier coefficients of the airgap force density waves. This concept can be used with different types of simulation blocks, such as analytical or numerical computation of e.g. forces or radiation patterns.

Despite the increasing requirements regarding the radiated audible noise of electric vehicles, practically acoustic aspects are not always considered from the beginning. Frequently, an electromagnetic design is not identified to be too loud until the layout is completed and a prototype has been constructed. This is an additional point of this paper. It will be shown how to extract sufficient data (transfer function and force excitation) from the electrical machine by comparatively simple means (microphone measurement, MATLAB, and electromagnetic 2D-FEM).

These data can then be used to optimize the acoustic performance of a PMSM drive in terms of electromagnetic noise excitations. Due to the transient character of the audible noise stemming from a variable speed drive, the chosen objective function has to account for that. One example used in this paper is to minimize the maximum sound pressure level (SPL) in dB(A) due to electromagnetic force excitations during the complete run-up of the machine with no mechanical load. It is shown how microphone measurements of a given prototype for the target application and numerical field calculation of the PM together with an analytical description of the stator slotting can be exploited to optimize the acoustic behavior of a variable speed PMSM. Virtual prototype refers here to the numerical simulation model in terms of structural dynamics and acoustic radiation, which has been validated for machines using the same manufacturing technology and having a similar size. The application of the proposed approach is limited here to the no-load case, because the studied device already showed high acoustic emission in this operation. Due to the minor influence of the stator slot geometry for distributed windings, the permanent magnet (PM) shape is considered to be the only optimization parameter. In principle however, the approach may be extended to optimize for full-load operation and include the stator slot geometry if required. In the given example, however, it is verified that also for the full-load case, the optimized design is quieter.

During the first half of the 20th century, Jordan introduced the idea that the interaction of electromagnetic force density waves with the mechanical and acoustic characteristics of the machine is the key to understanding and solving the problem of audible noise of electric machinery. In [1], Jordan uses the rotating field theory and derives formulas for the occurring ordinal numbers of the rotating field waves, calculates the eigenfrequencies and forced vibration of stators, treated as thin rings and even approximates the radiated acoustic power level of induction machines.

An early reference to address the forced vibration of electrical machines is dated to 1992 by Henneberger et al., who use 2D finite-element method (FEM) for numerically weak-coupling between electromagnetics and structural dynamics to compute the vibration of synchronous alternators [4]. At the end of the 1990ies, coupling electromagnetic and structural FEM in addition to an acoustic boundary element method (BEM) simulation became the standard

procedure [5][6][7][8]. For optimization purpose, the vibration response of the mechanical structure and the radiation characteristics can also be estimated using simple analytical formulas [9].

The influence of the PM shape on the electromagnetic force excitation and on the vibrational behavior of PMSM has been analyzed [10], e.g. radially magnetized magnets showed a frequency spectrum of force excitations with higher components at higher frequencies, due to the block shaped B-field. Block shaped magnets have a higher fundamental component and significantly less harmonics of higher order. Particularly in the case of tooth coil windings, the significance of the pole shape has been pointed out and exploited to optimize the vibrational behavior in the sense of torsional vibrations, i.e. reduction of cogging torque [11]. For tooth-coil windings, a partly enlarged air gap has been proposed as a measure for improving the acoustic behavior of PMSM [12]. In [13], the shape of interior PMs is optimized towards the minimum torque ripple. In addition to that, mechanical vibrations due to electromagnetic excitations are minimized in [14].

The influence of geometrical parameters of stator and rotor on the acoustic performance on a PMSM drive is investigated in [15], design-of-experiment methodology is employed to keep the number of necessary numerical simulations low. In contrast to this paper, the vibrational and acoustic behavior is assessed individually by means of a vibrational measurement (modal analyses) and an analytical radiation model. Vivier et al. use an analytical model for the magnetic circuit parameters and do not account for complicated magnet geometry.

The idea of FEM-to-measurement transfer function can also be found in [16]. In his thesis, Roivainen analyses the vibro-acoustic behavior of direct-torque-controlled (DTC) induction machines. Therefore, a structural dynamic analysis using unit-forces is performed. For verification purposes, the surface acceleration of the machine is measured and the unit-force transfer function is defined as the ratio of measured acceleration to simulated forces. Sound pressure measurements are not used for the measurement-to-FEM transfer functions.

The remainder of this paper is structured as follows: At first, the simulation methods and the underlying transfer function concept is introduced. A novel approach is introduced for the case if extensive simulations are not available, but prototype measurements are present. A section on the optimization potential regarding acoustic noise of electrical machines and aspects of auralization conclude this paper.

Simulation Methods

This work introduces the basic concepts to simulate signals of electrical drives for auralization. Auralization is a term used in analogy to the term visualization. It stands for a signal processing approach in which the engineer is enabled to listen to the results instead of just plotting third-octave band levels. In the following all required simulation steps are discussed in detail.

Transfer-function concept

A transfer-function-based approach is applied in this work. Amplitudes of force density waves are directly linked to the free-field sound pressure on an evaluation sphere surrounding the electrical machine. In this way, a separation into offline pre-calculation of structural and radiation data and an online-auralization becomes possible.

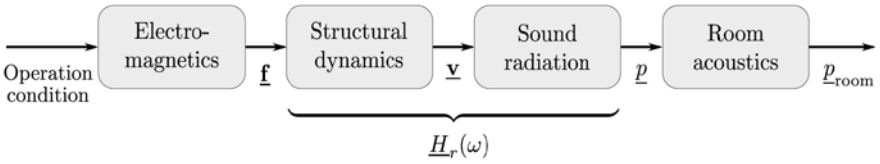

Figure 1: Schematic of transfer function-based simulation concept.

As shown in Figure 1, the proposed concept for the auralization of electrical machines consists of four simulation steps: The electromagnetic forces and the structural dynamic behavior are simulated by means of the FEM. The transfer function of the mechanical structure leads to a relation between the electromagnetic force **f** and the surface velocity **v**. The sound radiation simulation yields the transfer function from surface velocity **v** to sound pressure **p** at the evaluation points in the free-field. The room acoustic transfer function describes the sound propagation inside a room or car compartment from the source to a receiving position. This work only accounts for airborne sound transmission and shows the basic steps to simulate time signals for electrical drives in automotive applications. In order to include structure-borne sound transmission transfer paths have to be simulated or measured and integrated into the above-mentioned model.

In the same way as the force-to-velocity transfer function is expanded in a circumferential Fourier series called force modes *r*, there is also one transfer function from velocity to acoustic pressure per mode. The total transfer function from force to acoustic pressure is thus denoted $H_r(\omega)$ for each force mode *r*. For each observation point and for each mode *r*, a transfer function from force to acoustic pressure is calculated.

Electromagnetics

The electromagnetic excited audible noise is generated by harmonics of the air-gap field. Therefore, simple methods taking only the fundamental air-gap flux density wave into account are prohibited and more detailed approaches are needed. Nowadays, numerical methods such as the FEM are usually applied. They are characterized by a high level of detail in the model, such as non-linear material characteristics and exact description of the geometry, but they are computationally expensive. Especially in conjunction with parameter variations or geometrical optimization the FEM leads to unacceptably large computational costs. Therefore, a combination of analytical and FEM computation can be exploited, called hybrid modeling, making this simulation technique particularly interesting for the design and optimization of electrical drives in automotive industry. It is accurate in terms of the significant properties, still leading to a reduction of the computational costs. In the presented study, the acoustic radiation in no-load condition is of major interest. Therefore, the influence of saturation is negligible. Hence, analytic methods such as the conformal mapping approach are suitable for the air-gap field computation [17]. In general the solution is obtained by solving a linear Laplace problem, described by the geometry. The magnetic permeability is assumed to be linear, which results in a linear time invariant system consequently. This allows for an individual modeling of the stator slotting, permanent magnet field and the field of the coils. In the first step the slotting is modeled by means of a complex relative permeance function [17][18]

$$\underline{\lambda}(x) = \lambda^{\mathrm{rad}}(x) + \jmath\lambda^{\mathrm{azi}}(x) \tag{3}$$

where x denotes the angular position; $\lambda^{rad}(x)$ and $\lambda^{azi}(x)$ its radial and tangential component, respectively. In the next step the flux density of the surface-mounted permanent magnet is calculated considering a slot-less air gap. Since loaf shaped magnets are studied a separation of variables of the differential equation system is not possible, therefore a numerical solution is calculated. To reduce the computational effort, half a pole pitch is modeled by means of FEM and the radial and tangential air-gap flux density are gained by sampling. The entire field is reconstructed applying the symmetric properties of the machine and is described periodically on x from 0 to 2π by

$$\underline{B}_{\mathrm{pm}}(x) = B_{\mathrm{pm}}^{\mathrm{rad}}(x) + \jmath B_{\mathrm{pm}}^{\mathrm{azi}}(x), \tag{4}$$

The air-gap flux density for one revolution of the rotor can be calculated by circular time-shift of (4) and multiplication with (3):

$$\underline{B}_{\mathrm{slot}}(x,t) = \Re\left\{\underline{B}_{\mathrm{pm}}(x - 2\pi n \cdot t) \cdot \underline{\lambda}^{*}\right\}, \tag{5}$$

The permanent magnets are considered to have the magnetic permeability of air and do not effect the permeance function consequently. In Figure 2 the air-gap flux densities obtained by the hybrid model and by a full FEM are compared. The air-gap field of one pole pair is presented. The important harmonics of the air-gap field obtained by the hybrid model are in good agreement with the FEM solution. The surface force density acting on the stator teeth is calculated by means of the simplified Maxwell stress tensor

$$\sigma(x,t) = -\frac{\left(\underline{B}_{\mathrm{slot}}(x,t)\right)^2}{2\mu_0}, \tag{6}$$

where μ_0 is the magnetic permeability of vacuum. The flux density solution is calculated for one speed and the frequency and ordinal orders of the force density wave are used for the further investigation. The acceleration of the motor is considered in the total sound pressure calculation. With this approach the computational effort can be reduced from several hours to less then a minute for the simulation of one run-up, while the important aspects are modeled with a sufficient accuracy.

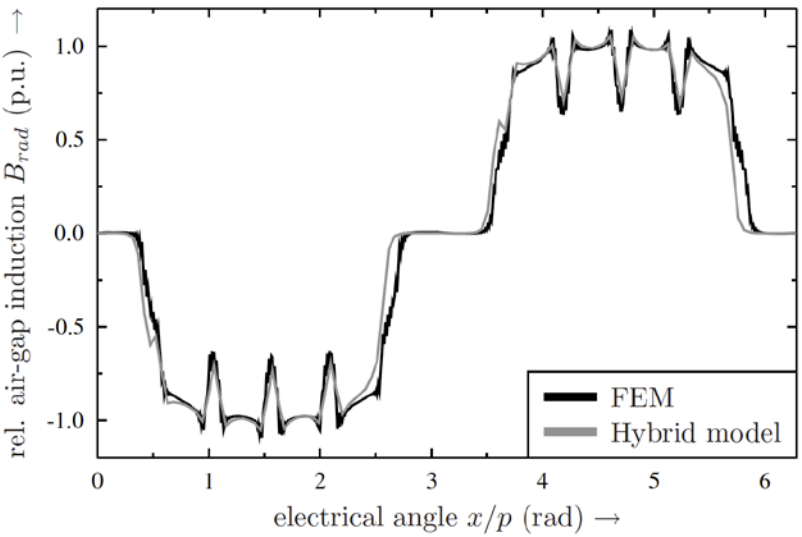

Figure 2: Comparison of air-gap flux-density: FEM and hybrid model.

Structural dynamics

A structural dynamics simulation connects simulated electro-magnetic forces and the surface velocity on the electrical machine. Commercial software packages can be used to process this simulation task by means of FEM simulations. Changes in the geometry directly require a re-run of the computationally extensive simulations. The determination of the material parameters has been found to be most critical in this step. The structural model of the electrical machine is shown in Figure 3. In this case the machine is air-cooled.

The results are organized in a way that the surface velocities are normalized to applied unit forces for each force mode *r*.

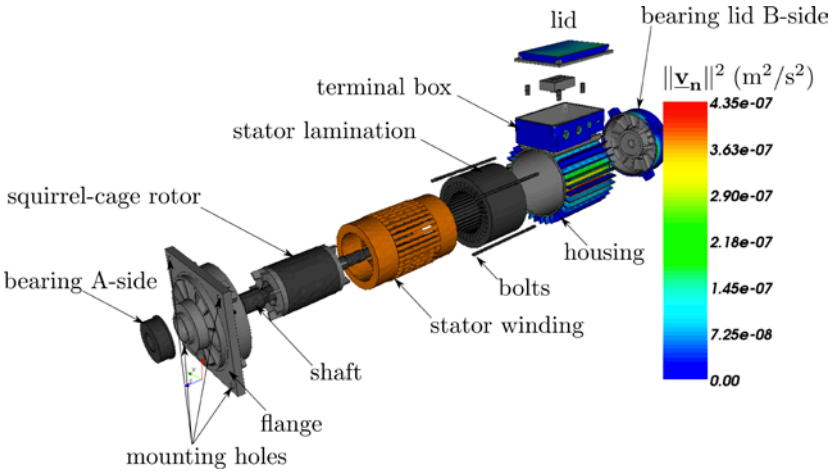

Figure 3: Mechanical model of the induction machine together with normal surface velocity on the housing at 533 Hz.

Sound Radiation

The free-field sound radiation of the electrical machine can be calculated by means of the Boundary Element Method. This method requires very long computation times if higher frequencies are considered [20]. Due to the geometry of electrical machines an analytic approach exploiting cylindrical harmonics can significantly reduce the computational costs as published by the authors [21]. However, we use a different approach using measurements and only electromagnetic simulations—structural dynamics and sound radiation are not simulated explicitly—as described in the section about the operational transfer function.

Results and Auralization

A PM synchronous machine is used as an example: The stator consists of a laminated sheet stack (M250-AP) with slots and the rotor is made from the same material and is equipped with surface-mounted permanent magnets ($\mu_r \approx 1$, $B_{rem} = 1.17$ T). The geometrical parameters are given in Table 1. The number of stator slots is $N_1 = 6$ and the number of magnets is $2p = 4$.
The transfer functions relating force densities to sound pressure are calculated. The resulting sound pressure distributions per unit-force are shown in Figure 6. It can be seen that even force orders cause a rotating velocity distribution where the radiation pattern of force order 3 indicates standing velocity distributions almost independent on frequency. Figure 5 shows the results of the unit-wave response-based approach: the sound power radiated by each force mode r.
In order to simulate a run-up, sweep signals are generated up to an order of 100. Thereby, the length of the signal is set to 5 s, start and end speeds are chosen to be 600 and 6000 min^{-1}. After the multiplication with the actual electromagnetic force density amplitudes, the resulting free-field sound pressure signal is obtained in 5 m distance. It is presented in form of a spectrogram shown in Figure 6.

Power Rating	750 W
Poles	2p = 4
Stator slots	36
Rotor slots	28
Q	3
Winding scheme	1/8/10/12

Rotor skewing	15 degrees
Mass	7.88 kg
Inner stator radius	35 mm
Outer stator radius	60 mm
Active length	80 mm
Total length	160 mm

Table 1: Specifications of the induction machine.

In the vicinity of certain eigenfrequencies of structural modes that are likely to be excited, the sound pressure increases significantly. In particular, those natural frequencies are located around 1, 2 and 4.5 kHz.

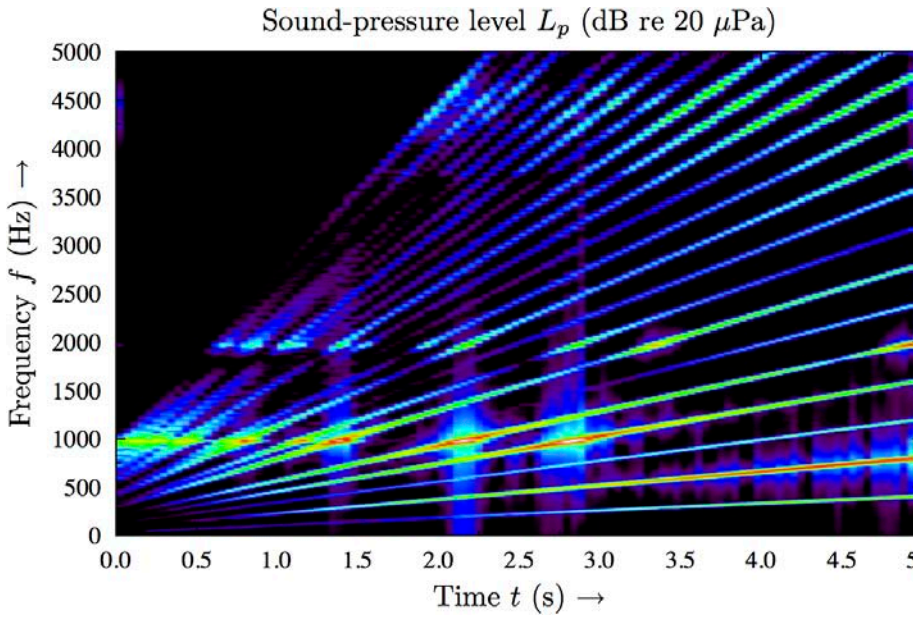

Figure 4: Spectrogram of a simulated run-up from 600 to 6000 min^{-1}.

In Figure 4, several order lines are visible. Each line is excited by a certain time-harmonic order, which is determined by the slope in the spectrogram, and by multiples of space orders. Despite this superposition of different space orders, one time harmonic order line is most commonly dominated by a single force space order.

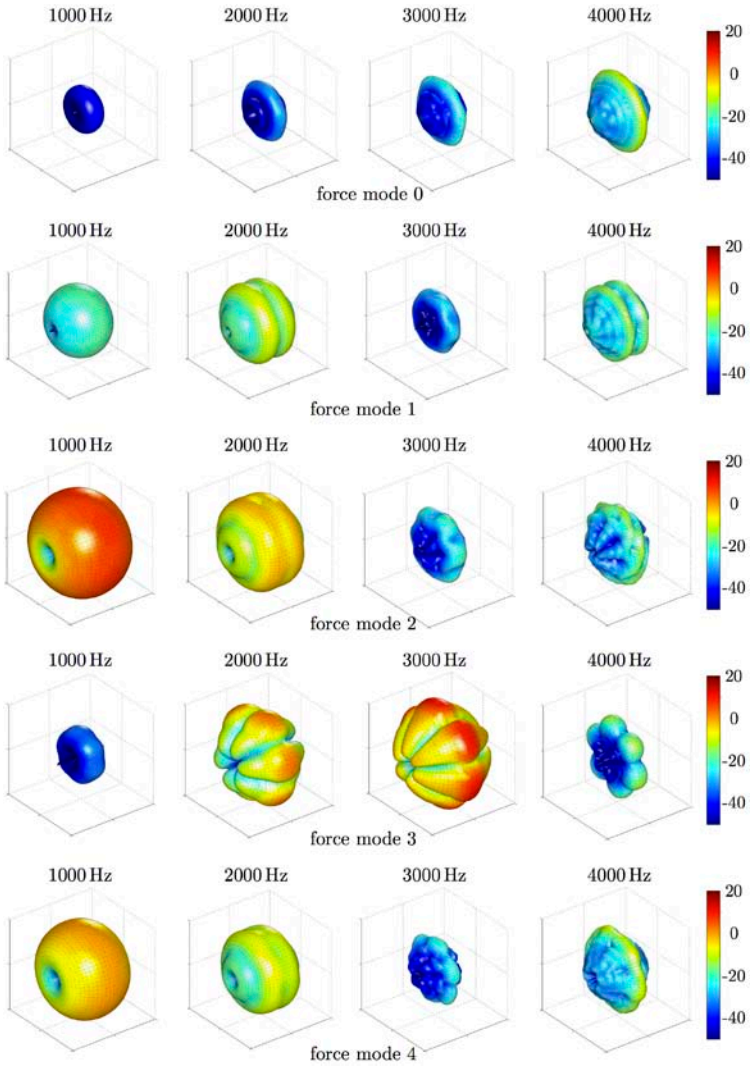

Figure 5: Sound-pressure level per unit-force in dB for radial force modes *r*.

Operational Transfer Function

As mentioned before, each block of the transfer function chain can be either investigated by analytical calculation, by numerical simulation or by measurements. In this sense, there is a signal (and energy) flow from current/PM excitation, via flux density and reluctance forces, through surface velocity to sound pressure and particle velocity. For each of the three parts a transfer function can be defined, where the transfer function of the latter two typically can be considered being linear. For example, the mechanical transfer function can be determined by means of numerical modal analysis (using FEM) or by means of experimental modal analysis (using shaker, accelerometer and dual-spectrum analyzer), for a point excitation.

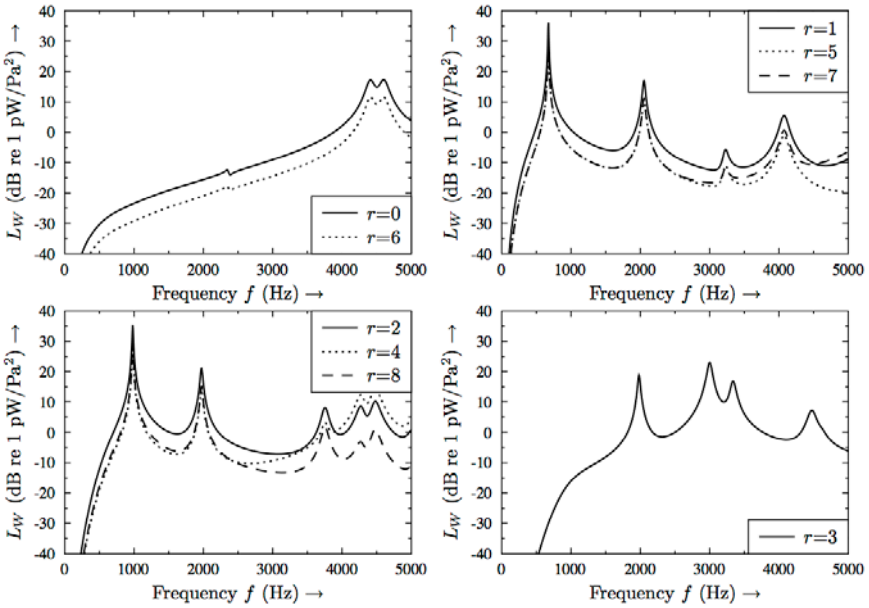

Figure 6: Sound power level per unit force mode *r*.

Alternatively to defining the transfer function purely from measurement, or purely from simulation and under the assumption that the operating conditions are approximately equal, we can define a mixed formulation for the transfer function as

$$H = \frac{B_{\text{meas}}}{A_{\text{simu}}}, \tag{7}$$

where B_{meas} is the measured output of the transfer function, and A_{simu} is the simulated input. Using magnetic forces as A_{simu} is a good choice for two reasons: First they can be simulated comparatively accurately using 2D-FEM and secondly they are very difficult to be measured. In [16], B_{meas} is chosen to be the surface acceleration and A_{simu} is indeed the magnetic force. In this paper, the transfer function is chosen to include the path up to the sound pressure. The idea of this formulation of the transfer function has been deduced from the well known operational modal analysis, and is therefore considered to be a valid approach.

The starting point for the determination of transfer functions is a microphone measurement of sound pressure $p_{\text{meas}}(t)$ and a synchronized speed measurement $n(t)$ during an unloaded run-up of the PMSM with sufficiently slow slew rate. This is mapped to a so called spectrogram given by $p_{\text{meas}}(\omega, n)$, which shows dominant lines due to harmonic force excitations. Using a peak-picking technique along these lines, allows for the definition of lines of constant order k as $p_{\text{meas}}(\omega,k)$, $k=\omega /(2\pi n)$.

As a second step, it is essential to trace back each order line to a specific harmonic. This can either be done using standard table works [1], or in more sophisticated manner by tracing back to individual field harmonics [24]. The latter detailed approach is not necessary for the method proposed in this paper, it however may reveal more insight and may help trouble shooting the computer routines. For the unloaded run-up, the space vector diagrams are flat, i.e. there is no imaginary component of the force waves, due to the absence of stator currents. The Fourier decomposition of the reluctance-force-density waves reads

$$\sigma(x,t) = \sum_{k=1}^{K} \sum_{r=-R}^{R} \hat{\sigma}_{rk} \cos(rx + k \cdot 2\pi n \cdot t + \varphi)\,. \tag{8}$$

Now the assumption is made, that one harmonic force wave given by frequency harmonic number *k'* and by wave number *r* is dominant and solely accounted for at one line of constant order. Then, the FEM-to-measurement transfer function is defined as

$$H_r(\omega) = \left. \frac{p_{\text{meas}}(\omega, k)}{\hat{\sigma}_{rk}} \right|_{k=k'}, \tag{9}$$

where $\hat{\sigma}_{rk}$ is determined from a FEM simulation of the very geometry as the prototype delivering sound pressure measurements $p_{\text{meas}}(\omega,k)$. The SPL for a given force excitation $\tilde{\sigma}_{rk}$ can be calculated by means of superposition:

$$L_p(\omega, n) = 20 \log \left(\sum_{k=\frac{\omega}{2\pi n}}^{K} \sum_{r=-R}^{R} \frac{\tilde{\sigma}_{rk} \cdot H_r(\omega)}{p_{\text{ref}}} \right) - \Delta_A(\omega) \tag{10}$$

where $p_{\text{ref}}=20\mu$Pa. However, all results presented in this paper are referred to a slightly different reference pressure leading to an undisclosed offset in all level plots due to reasons of confidentiality.

To compensate for the frequency dependency of the human ear, measured or simulated audible signals are passed through a filter, of which the *A* filter is the most common. Therefore, (10) gives the unweighted pressure level in dB, if $\Delta_A = 0, \forall \omega$ and it gives SPL in dB(*A*), if the *A* filter values are used for $\Delta_A(\omega)$.

The quadratic pressure levels of incoherent signals may be summed up immediately. Therefore, the (A-weighted) total SPL is then given by

$$L_{p,\text{tot}}(n) = 10 \log \sum_{l=1}^{N} 10^{L_p(l\omega_0, n)/10} \tag{11}$$

in dB(*A*), where ω_0 corresponds to the window, which was initially used to determine $p_{\text{meas}}(\omega,2\pi n)$. The next section is devoted to the question, how to calculate $\hat{\sigma}_{rk}$ efficiently for various PM shapes and speeds.

Optimization

Due to the excited single tones in its audible spectrum, the electromagnetic excited noise is the most unpleasant contribution. Therefore, the reduction of electromagnetic noise excitation is the classical approach to a low noise design of electrical machines. All activities to damp structural vibration and to suppress radiation are typically secondary measures. If a machine is to be designed with special requirements to noise and vibration or if an existing design should be improved in this respect, there are several setscrews that can be divided into five different categories:

1) Main dimensions and numbers, such as number of poles, slots, etc.
2) Micro-geometry, e.g. of the stator slots, permanent magnet shape, pole shape, etc.
3) Winding, i.e. distribution, cording, parallel paths, etc.
4) Supply, i.e. switching frequency, control, etc.
5) Manufacturing, including tolerances, assembly, etc.

The parameters of influence can be further distinguished between their physical effects, i.e. whether it excites (current density or permanent magnet) or guides (permeance) the field.

The given example concentrates on the micro-geometry, i.e. on the shape of the permanent magnet whereat the optimization starts at an undisclosed reference geometry. This geometry is defined by three parameters (*H, W, R*) as shown in Figure 7.

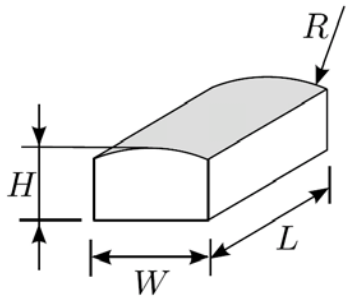

Figure 7: Geometrical definition of magnet shape [25].

Additionally, the mechanical air-gap length δ is varied. The axial length of the magnet is equal to that of the active length of the machine and is kept constant. The objective of the optimization in this study is to reduce the maximum occurring total SPL during a run-up. Therefore, the objective function is defined as

$$f(H, W, R, \delta) = \max_n L_p \rightarrow \min. \tag{12}$$

The optimization problem is to find a combination *(H, W, R, δ)* that minimizes *f* under manufacturability boundary constraints. The flux density in the air gap was used as an additional constraint (95% to 110%), in order to obtain a similar mean drive torque, which has to be verified after the optimal design is found. Since the computation time of the hybrid approach is very low, the four-dimensional parameter space is discretized between the min/max values and the objective function is computed for every combination of *H, W, R* and *δ*. Table 1 gives a comparison between the reference design and the optimized design as well as minimum and maximum values. As can be seen, the maximum occurring total SPL is reduced by approx. 9 dB(*A*). This is achieved on the expense of more PM material, as the cross sectional area is 26 % higher the fundamental flux density wave is increased by 17 %. The relative price of the machine is evaluated according to the material effort, assuming a price of 80 Euro/kg for the PM material, 15 Euro/kg for the copper wires and 5 Euro/kg for the soft magnetic steel sheets. Taking the volume ratios into account this gives rise to an increase of the machine price of approx. 5 %.

The simulated A-weighted SPL obtained from the hybrid model applying the FEM-to-measurement transfer function for both geometries (original and optimized) is compared in Figure 8. It shows that high values of total sound pressure at high speeds (reference geometry) are traded for comparatively higher values in the interval between 300 and 400 Hz, but still leading to the reduction of approx. 9 dB(*A*). There is a slight difference between maximum SPL from the hybrid model and from FEM. However, the difference is not significant, since the tendency between optimized and reference geometry matches.

Quantity	Min	Max	Reference	Optimized
Magnet height *H*	83 %	133 %	100 %	120 %
Magnet width *W*	78 %	117 %	100 %	111 %
Magnet radius *R*	85 %	115 %	100 %	84 %
Air-gap length _	83 %	117 %	100 %	117 %
Cross sectional area of PM			100 %	126 %
Magnet-pitch to pole-pitch			80 %	88 %
Fundamental flux density B	95 %	110 %	100 %	101 %
THD of air gap flux density			35 %	11 %
Mean torque T_{mean}			100 %	101 %
Torque ripple			4.03 %	2.96 %
Max. total SPL L_p (dB(A))			70	61

Table 2: COMPARISON OF REFERENCE AND OPTIMIZED GEOMETRY.

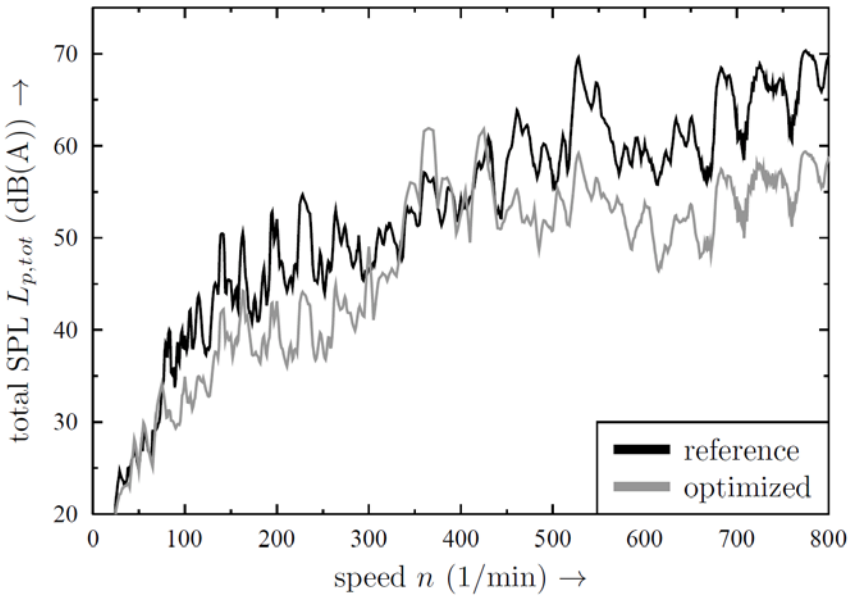

Figure 8: Simulated sound power level, comparison between reference and optimized design.

Conclusions and Future Perspective

Basic simulation steps for the calculation of time signals of electrical machines for automotive applications have been introduced. A transfer-function based approach allows for independent calculations of the different domains: electro-magnetics, structural-dynamics and sound radiation. An engine run-up including the structural response of the machine housing has been simulated. The results show great potential for the designer of electrical-drives, especially for automotive industry, where the acoustic performance has an impact on the acceptance of the car by the customers.

A novel approach in this field—combining electro-magnetic simulations and sound pressure measurements on a prototype—leading to an operational transfer function has been introduced. Based on measurements on an exemplary electrical drive the acoustic performance has been analyzed using this technique yielding in a significant reduction of radiated sound pressure levels by modification of the shape of the magnetic material for an entire machine run-up.

In a next step a standard automotive operation cycle including different load conditions can be simulated. By further including measured or simulated air-borne as well as structure-borne transfer functions, and if necessary, a room acoustic simulation of the car compartment, binaural sound signals at the driver's ear can be obtained [18]. Employing in addition to the acoustic model an optical model of the car, allows for the immersion into a virtual reality scenario in which the acoustic performance of an electrical driven car can be analyzed.

References

[1] uscharme Elektromotoren. W. Girardet, November 1950.

[2] M. Ruhdorfer, smart fortwo electric drive, ADAC autotest, September 2010

[3] G. Stegmaier, Tesla Roadster – Der elektrische Kolbenfresser, FOCUS-Online, 2008

[4] G. Henneberger, P. Sattler, W. Hadrys, and D. Shen, "Procedure for the numerical computation of mechanical vibrations in electrical machines," IEEE Transactions on Magnetics, vol. 28, no. 2, pp. 1351–1354, March 1992.

[5] C. Neves, R. Carlson, N. Sadowski, J. Bastos, N. Soeiro, and S. Gerges, "Calculation of electromagnetic-mechanic-acoustic behavior of a switched reluctance motor," IEEE Transactions on Magnetics, vol. 36, no. 4, pp. 1364–1367, 2000.

[6] M. Furlan, A. Cernigoj, and M. Boltezar, "A coupled electromagnetic- mechanical-acoustic model of a DC electric motor," COMPEL: The International Journal for Computation and Mathematics in Electrical and Electronic Engineering, vol. 22, no. 4, pp. 1155–1165, 2003.

[7] C. Wang, J. Lai, and A. Astfalck, "Sound power radiated from an inverter driven induction motor II: Numerical analysis," IEE Proceedings Electric Power Applications, vol. 151, pp. 341–348, May 2004.

[8] M. van der Giet, E. Lange, D. A. P. Correa, I. E. Chabu, S. I. Nabeta, and K. Hameyer, "Acoustic simulation of a special switched reluctance drive by means of field circuit coupling and multiphysics simulation," IEEE Transactions on Industrial Electronics, vol. 57, no. 9, pp. 2946 – 2953, 2010.

[9] J. Le Besnerais, A. Fasquelle, M. Hecquet, J. Pelle, V. Lanfranchi, S. Harmand, P. Brochet, and A. Randria, "Multiphysics modeling: Electro-vibro-acoustics and heat transfer of pwm-fed induction ma- chines," IEEE Transactions on Industrial Electronics, vol. 57, no. 4, pp. 1279 –1287, 2010.

[10] G. Jang and D. Lieu, "The effect of magnet geometry on electric motor vibration," IEEE Transactions on Magnetics, vol. 27, no. 6, pp. 5202 –5204, November 1991.

[11] K.-J. Han, H.-S. Cho, D.-H. Cho, and H.-K. Jung, “Optimal core shape design for cogging torque reduction of brushless dc motor using genetic algorithm,” IEEE Transactions on Magnetics, vol. 36, no. 4, pp. 1927– 1931, 2000.

[12] Y.Asano,Y.Honda,H.Murakami,Y.Takeda,andS.Morimoto,“Novel noise improvement technique for a PMSM with concentrated winding,” in Proceedings of the Power Conversion Conference, PCC Osaka 2002, vol. 2, 2002, pp. 460–465 Vol.2.

[13] S.-I. Kim, J.-Y. Lee, Y.-K. Kim, J.-P. Hong, and Y.-H. Jung, “Optimiza- tion for reduction of torque ripple in interior permanent magnet motor by using the Taguchi method,” IEEE Transactions on Magnetics, vol. 41, no. 5, pp. 1796 –1799, May 2005.

[14] G.-H. Kang, J. Hur, W.-B. Kim, and B.-K. Lee, “The shape design of interior type permanent magnet BLDC motor for minimization of mechanical vibration,” in IEEE Energy Conversion Congress and Exposition, ECCE 2009, September 2009, pp. 2409 –2414.

[15] S.Vivier, M. Hecquet, A. Ait-Hammouda, P.Brochet, “Experimental design method applied to a multiphysical model trellis designs for a multidimensional screening study,” COMPEL: The International Journal for Computation and Mathematics in Electrical and Electronic Engineering, vol. 24, no. 3, pp. 726–739, 2005.

[16] J. Roivainen, “Unit-wave response-based modeling of electro mechanical noise and vibration of electrical machines,” Ph.D. dissertation, Helsinki University of Technology, 2009.

[17] D. Zarko, D. Ban, and T. Lipo, “Analytical calculation of magnetic field distribution in the slotted air gap of a surface permanent-magnet motor using complex relative air- gap permeance,” IEEE Transactions on Magnetics, vol. 42, no. 7, pp. 1828–1837, 2006.

[18] M. Vorländer, “Auralization – Fundamentals of Acoustics, Modelling, Simulation, Algorithms and Acoustic Virtual Reality”, Springer Berlin, 2007

[19] M. Hafner, D. Franck, and K. Hameyer, “Static electromagnetic field computation by conformal mapping in permanent magnet synchronous machines,” IEEE Transactions on Magnetics, vol. 46, no. 8, pp. 3105 –3108, August 2010.

[20] M. Aretz, L. Jauer, M. Vorländer, “Sound field simulations in a car passenger compartment using combined finite element and geometrical acoustics simulation methods”, Aachen Acoustic Colloquium, November 2009.

[21] M. Müller-Trapet, P. Dietrich, M. van der Giet, J. Blum, M. Vorländer, K. Hameyer, “Simulated Transfer Functions for the Auralization of Electrical Machines”, EAA Euroregio Congress on Sound and Vibration, 2010

[22] M. van der Giet, M. Müller-Trapet, P. Dietrich, M. Pollow, J. Blum, K. Hameyer, M. Vorländer, “Comparison of acoustic single-value parameters for the design process of electrical machines”,39th International Congress and Exposition on Noise Control Engineering – Internoise, 2010

[23] M. van der Giet, J. Blum, P. Dietrich, S. Pelzer, M. Müller-Trapet, M. Pollow, M. Vorländer, K. Hameyer , “Auralization of electrical machines in variable operating conditions”, IEEE International Electric Machines and Drives Conference (IEMDC), 2010

[24] M. van der Giet, “Analysis of electromagnetic acoustic noise excitations: A contribution to low-noise design and to the auralization of electrical machines”, PhD thesis, RWTH Aachen, 2011

[25] M. van der Giet, D. Franck, R. Rothe, and K. Hameyer, “Fast-and-easy acoustic optimization of PMSM by means of hybrid modeling and FEM-to-measurement transfer functions,” in 2010 XIX International Conference on Electrical Machines (ICEM), 2010, pp. 1 –6.

[26] VACOMAX VACODYM, Vacuumschmelze, P.O. Box 2253 Grüner Weg 37 D 63412 Hanau, Germany.